



Supporting Online Material for

Glia Promote Local Synaptogenesis Through UNC-6 (Netrin) Signaling in *C. elegans*

Daniel A. Colón-Ramos, Milica A. Margeta, Kang Shen*

*To whom correspondence should be addressed. E-mail: kangshen@stanford.edu

Published 5 October 2007, *Science* **318**, 103 (2007)

DOI: 10.1126/science.1143762

This PDF file includes:

Materials and Methods
Figs. S1 to S9
References

Materials and Methods

Strains and genetics

Worms were raised on NGM plates at 22°C using OP50 *E. coli* as a food source. N2 Bristol was utilized as the wild-type reference strain (34). The following mutant strains were obtained through the *Caenorhabditis* Genetics Center: MT324 *unc-40(n324)I*, CB271 *unc-40(e271)*, and NW434 *unc-6(ev400)X*. NG3072 *unc-34(gm104)V* was a kind gift from Dr. Gian Garriga at University of California at Berkeley, and LE983 *unc-34(lq17)V* was a kind gift from Dr. Erik Lundquist at University of Kansas.

Molecular biology and transgenic lines

Expression clones were made in the pSM vector, a derivative of pPD49.26 (A. Fire) with extra cloning sites (S. McCarroll and C.I. Bargmann, unpublished data). The plasmids and transgenic strains (10-120ng μl^{-1}) were generated using standard techniques and coinjected with markers *Punc-122::GFP* or *dsRED* (20-30ng μl^{-1}): *wyls45(Pttx3::gfp::rab3)*, *wyEx1262 [Pttx-3::gfp, Pglr-3::mCherry]*, *wyEx1273 [Pttx3::cfp::rab3, Pglr-3::glr-1::yfp, Phlh-17::mCherry]*, *wyEx1126 [Punc-6::unc-6, Phlh-17::mCherry]*, *wyEx800 [Pttx-3::mCherry, Pglr-3::mCherry, Punc-40::unc-40]*, *wyEx1474 [Pttx-3::mCherry, Pcex-1::mCherry, Punc-40::unc-40]*, *wyEx1523 [Pttx-3::mCherry, Pcex-1::mCherry, Punc-40::unc-40::sl2::yfp]*, *wyEx1150 [Pttx-3::mCherry::rab-3, Pttx-3::unc-40::gfp]*, *wyEx1149 [Pttx-3::mCherry::rab-3, Pttx-3::unc-40::gfp]*, *wyEx1770 [Pglr-3::mCherry, Pcex-1::mCherry, Punc-40::unc-40::sl2::yfp]*, *wyEx1825 [Pttx-3::syd-2]*, *wyEx1961*

[*Pttx-3::myr-GFP, Pttx-3::mCherry::rab3*], *wyEx496* [*Pttx3::mCherry::rab3, Pttx-3::elks-1::yfp, Pttx-3::cfp*]. Detailed subcloning information will be provided upon request.

Fluorescence microscopy and confocal imaging

Images of fluorescently tagged fusion proteins were captured in live *C. elegans* using a Plan-Apochromat 63X/1.4 objective on a Zeiss LSM510 confocal microscope system. Visual inspections and some quantifications were done using a Zeiss Axioplan 2 microscope with Chroma HQ filter sets for GFP, YFP, CFP and RFP (63X/1.4NA objective). Worms were immobilized using 10mM levamisole (Sigma) and oriented anterior to the left and dorsal up. Volume rendering was done using the software OsiriX.

Genetic screens

unc-40(wy81) was isolated from a visual screen of 900 haploid genomes in AIY interneuron for mutants with defects in RAB-3::GFP distribution in Zone 2. Animals were mutagenized with EMS in this screen.

Quantification and mosaic analysis

Quantification of the synaptic distribution in AIY was performed by measuring the relative distribution of fluorescence intensity in confocal micrographs.

Fluorescence intensity was measured using the line scan function of ImageJ and tracing the AIY process. To measure the percentage of fluorescence intensity in

Zone 2, Zone 2 was morphologically defined as a 5 μ m region of the AIY process which encompasses the dorsal turn as the process exits the anterior ventral nerve cord and enters the nerve ring (boxed in all figures). Total fluorescence intensity in this region was divided by total fluorescence intensity for Zone 2 and 3, which yielded the percentage of fluorescence intensity in Zone 2.

The axonal width of Zone 2 and Zone 1 was measured in wild type and *unc-40* animals by defining Zone 2 as described above, and measuring the widest area of Zone 2 and the widest proximal region of Zone 1. These areas were selected because they corresponded to those presented as “Cross-section A” (Zone 2) and “Cross-section D” (Zone 1) in the AIY diagram of the studies published in *The mind of the worm* (5). Measurements of the confocal micrographs were conducted by using the overlay measurement function of the LSM Image browser software. Measurements for the axonal width of the electron micrographs were conducted by measuring the width of the axon of AIY in cross-sections in the animal JSH (WormImage. David Hall and Huawei Weng (2006) www.wormimage.org). AIYL and AIYR were identified and their width were quantified using ImageJ for Zone 2 (sections 255-260) and Zone 1 (sections 300, 313, 323, 334, 344 and 355).

Mosaic analysis was conducted on *unc-40(e271)* or *unc-40(n324)* animals expressing unstable transgenes with a *unc-40* rescuing construct, and cytoplasmic cell-specific markers in RIA and AIY, or RIB and AIY (*wyEx 800* and *wyEx1474* respectively). Animals were inspected for retention of the transgene using a Zeiss Axioplan 2 microscope. Mosaic analysis for AIY presynaptic

patterning was done by scoring animals for rescue of presynaptic vesicle distribution in AIY, as defined by an enrichment of presynaptic vesicles in Zone 2, and discrete synaptic clusters in Zone 3. Mosaic analysis for RIA axon guidance was done in a similar manner, but animals were scored for rescue of RIA guidance as defined by the process correctly entering the nerve ring sub-dorsally, running ventrally towards Zone 2, looping around the ventral ganglion neuropile, reentering the nerve ring on the ipsilateral side and circumnavigating the nerve ring dorsally. Only when all these decisions were made correctly were animals scored as rescued. Mosaic analysis in *unc-6* animals was performed in a similar manner to that of *unc-40* animals except that array retention was tracked in the ventral versus the dorsal cephalic sheath cells in *unc-6 (ev400)* animals. Quantification of the distribution of UNC-40::GFP in the AIY process, and quantification of the position of the sheath cell end-feet, RIA axon guidance and AIY presynaptic distribution was done by inspecting and scoring animals using the Zeiss Axioplan 2 microscope. Statistical significance was calculated using Student's t-test or chi squared.

Identification of the RIB neurons

The promoter region of the *cex-1* gene was used to drive the expression of mCherry. One pair of bilaterally symmetric head neurons was clearly labeled in the *wyEx1474* animals. The cell bodies of these neurons are localized in the lateral ganglion. Their axons first migrate ventrally and then around the nerve ring. We identified these cells as RIB based on the morphological features of the axon. There were two morphological features that suggested these cells to be

RIB: 1) the labeled axons stop at the dorsal midline and 2) the presence of branches on the nerve ring portion of the axons. Other groups have identified these cells as RIMs based on the cell body position using Differential Interference Contrast microscopy (Cori Bargmann, Personal Communication). The interpretation of the mosaic results will not be significantly different regardless of whether the cells are RIMs or RIBs since both RIMs and RIBs are more closely related to AIY than the RIA neurons. Therefore, the RIB/RIM mosaics are more stringent than the RIA mosaics.

Reference:

29. Z. Gitai, T. W. Yu, E. A. Lundquist, M. Tessier-Lavigne, C. I. Bargmann, *Neuron* **37**, 53 (Jan 9, 2003).
30. E. Yeh, T. Kawano, R. M. Weimer, J. L. Bessereau, M. Zhen, *J Neurosci* **25**, 3833 (Apr 13, 2005).
31. J. E. Sulston, E. Schierenberg, J. G. White, J. N. Thomson, *Dev Biol* **100**, 64 (Nov, 1983).
32. Z. Altun-Gultekin *et al.*, *Development* **128**, 1951 (Jun, 2001).
33. J. A. Zallen, S. A. Kirch, C. I. Bargmann, *Development* **126**, 3679 (Aug, 1999).
34. S. Brenner, *Genetics* **77**, 71 (May, 1974).

Suppl. Fig. 1 AIY axon morphology is similar between wild type and *unc-40* mutants. **(A-L)** Confocal micrographs of representative wild type animals (A-C and G-I) or *unc-40* animals (D-F and J-L) coexpressing myristoylated GFP and mCherry::RAB-3 (A-F) or cytoplasmic CFP and mCherry::RAB-3 (G-L). Scale bars, 5 μ m. **(M)** Diagram of a reconstruction of AIY morphology and presynaptic site distribution based on serial EM micrographs generated by (5). The arrows indicate the presynaptic specializations documented by White and colleagues

during their reconstruction of the worm nervous system(5). Note the asynaptic Zone 1 and the high concentration of presynaptic specialization is Zone 2. Furthermore, in Zone 3, White and colleagues document that AIY formed between 4-8 interspersed presynaptic specializations, none of which innervated RIA. The EM data strongly correlates with that observed using our synaptic markers, which also show that Zone 1 is an asynaptic region and that Zone 2 has a large concentration of presynaptic specializations. Furthermore, our synaptic markers label precisely 4-8 presynaptic clusters in Zone 3, as reported by White and colleagues, and none of these presynaptic markers are in contact with RIA, suggesting that they are not innervating RIA in Zone 3 (see also Figure 1 and 2). The correlation between our synaptic markers and the EM studies is consistent with other published reports, which have shown that similar synaptic markers display exquisite sensitivity and faithfully represent, *in vivo*, the synaptic patterning observed in the fixed EM cross-sections(28). **(N-O)** Two representative electron micrographs of Zone 1 region (N) and Zone 2 region (O) in the same wild type organism. AIY is pseudocolored red, while AIY postsynaptic partners are pseudocolored green and the sheath cell, blue. Note the dramatic difference of the size and shape of AIY between Zone 2 and Zone 1. Zone 2 has large axon diameter and complex irregular morphology, while Zone 1 is significantly smaller in size and has simple round shape. Zone 2 is a highly enriched presynaptic region as determined by the presence of both electron-dense active zone structures and synaptic vesicles. Also note the ventral cephalic sheath cell process adjacent to the AIY presynaptic rich region in

Zone 2 (modified and reproduced with permission from David Hall and Huawei Weng (2006) <<http://www.wormimage.org>>www.wormimage.org and from the original work of(5)). Scale bars, 500nm. **(P-R)** Quantification of the axon width in Zone 1 or Zone 2 region in a wild type (P, columns to the left in Q) or *unc-40* animal (columns to the right in Q) visualized by EM (P) or by cytoplasmic GFP (Q). Note that the measurements using EM and fluorescence markers closely agree with each other both in terms of AIY axon morphology and presynaptic distribution. Notably, Zone 2 (dashed box) is a synaptic rich region, which is significantly wider than a nearby asynaptic region (Zone 1). Interestingly in *unc-40* mutants, in which we observe a reduction of presynaptic specializations in Zone 2, we also observe a reduction in the average width of the Zone 2 region compared to wild type animals. This is consistent with the notion that *unc-40* animals have reduced presynaptic specializations in Zone 2. This change is not likely due to general morphological changes because the width of nearby asynaptic Zone 1 region does not change.

Suppl. Fig. 2 *wy81* is an allele of *unc-40*. **(A)** Confocal micrograph demonstrating the localization and patterning of AIY presynaptic vesicles (GFP:RAB-3 and pseudocolored red) in a representative *wy81* animal. Genetic mapping and complementation revealed that *wy81* is an allele of *unc-40*, as *wy81* failed to complement the putative null alleles of *unc-40*, and *wy81* phenotype could be rescued by expressing a transgene containing the *unc-40* open reading frame under its endogenous promoter (data not shown). **(B)** *unc-*

40 encodes a type I transmembrane protein with 1415 residues. Its ectodomain has four V-like immunoglobulin modules (dark green) and six fibronectin type III modules (light green), followed by a transmembrane α helix (blue) and a large cytoplasmic domain with three conserved regions (dark green boxes) (6, 29). Sequence analysis revealed that *wy81* changes the E221 codon to a UAA stop codon, causing a premature stop in the second V-like immunoglobulin module. Also shown are other published putative *unc-40* alleles. *e1430* changes the R157 codon to a UGA stop, and is not thought to make a functional product. *n324* changes L444 to a UAA stop (6). Scale bars, 5 μ m.

Suppl. Fig. 3 Axon guidance of AIY and RIA in *unc-40* animals. **(A-L)** Confocal micrograph of a representative wild type animal (A-F) or an *unc-40* animal (G-L) expressing cytoplasmic fluorophores in AIY (pseudocolored red) and RIA (pseudocolored green). 3-D reconstructions of the confocal sections were rotated to show the circumnavigation of AIY and RIA at the nerve ring (D-F; J-L). White arrow at the top of the micrograph column indicates position of the anterior end of the animal. All images are oriented dorsal facing up and ventral, down (as indicated by the black arrowhead to the left of (A)). White arrowhead in (D and J) indicates the precise site where the two AIY interneurons meet after successfully concluding all of their axon guidance decisions. **(M)** Quantification of the axon guidance decisions made by AIYs in wild type (blue, n= 26 neurons) or *unc-40* animals (red, n=36 neurons). We examined the three navigational decisions AIY makes as it traverses the ventral nerve cord and the nerve ring: 1) Initially, its

process exits the ventral ganglion where the AIY cell body resides and projects anteriorly along the ventral nerve cord (scored as “Decision 1”), 2) upon encountering the nerve ring, it turns dorsally and enters the nerve ring (scored as “Decision 2”); and 3) it then circumnavigates the periphery of the nerve ring until it reaches the dorsal midline, where it precisely touches the tip of its bilaterally symmetric AIY partner (scored as “Decision 3”). The only axon guidance defect scored in the examined cells was a 7% axon truncation defect. (N)

Quantification of the axon guidance decisions made by RIAs in wild type (blue, n= 26 neurons) or *unc-40* animals (red, n=34 neurons). We examined the two major navigational decisions RIA makes as it traverses the ventral nerve cord and the nerve ring: 1) the process enters the nerve ring sub-dorsally, runs ventrally towards Zone 2, loops around the ventral ganglion neuropil and reenters the nerve ring on the ipsilateral side (scored as “Decision 1”); 2) upon reentering the nerve ring, the process circumnavigates the nerve ring dorsally (scored as “Decision 2”). Axon guidance in RIA was affected in *unc-40* animals: RIA failed to make decision 1 correctly and contact AIY in Zone 2. Interestingly, although RIA fails to make decision 1 correctly, once the RIA process reaches the nerve ring RIA guidance resumes normally, circumnavigating the nerve ring as in wild type animals. Our data suggests that RIA guidance decisions are modular, and that *unc-40* is not necessary for all guidance decisions in RIA. Scale bars, 5 μ m

Suppl. Fig. 4 UNC-40/DCC affects localization of SYD-2/liprin α . (A, B)

Confocal micrographs showing the distribution of SYD-2/liprin α in AIY in wild

type (A) or *unc-40* (B) animals. SYD-2/liprin α is a member of a conserved family of proteins that regulate active zone morphology. This protein has been shown to localize strictly to active zones, and has been used as an active zone marker (30). A significant reduction of fluorescence intensity in Zone 2 of *unc-40* animals lends further credence to the hypothesis that UNC-40 is required for correct presynaptic patterning in AIY. Scale bars, 5 μ m.

Suppl. Fig. 5 Lineage relationships of AIY. **(A)** Lineage diagram showing the relationship between RIA, RIB and AIY. Note that RIB is more closely related to AIY than RIA is to AIY. Divergence in their lineages is indicated in red in the lineage name for each of the three cells. Shown here is the lineage diagram for AIYL, but the lineage diagram for AIYR is similar (31). **(B-C)** Tables describing the cells closely related to AIYL (B) or AIYR (C). The (X) symbol represents presence of the neuron in the indicated anatomical areas, while the (-) symbol indicates that the neuron is not normally present in that anatomical areas. These are the only cells in the *C. elegans* lineage more closely related to the AIY neurons than the RIB neurons, and therefore, the only cells for which the RIB mosaic analysis could not account. Out of these cells, the only cell(s) that are present in the Zone 2 region are RMEV and RIH. Yet, while we know that UNC-40/DCC is expressed in AIY, we have no evidence that RMEV or RIH express UNC-40/DCC.

Suppl. Fig. 6 UNC-40/DCC acts cell-autonomously in AIY to pattern AIY presynapses. **(A-C)** Expression in *unc-40* animals of a bicistronic construct that contains the endogenous *unc-40* promoter driving the *unc-40* cDNA followed by a SL2 splice receptor and YFP. Expression of YFP in this bicistronic construct tracks *unc-40* endogenous expression, which was observed in several head neurons (A). Simultaneous cell-specific expression of a cytoplasmic fluorophore in AIY and RIB (B) demonstrated that UNC-40/DCC is endogenously expressed in AIY (C). **(D-O)** Confocal micrographs of representative animals belonging to the four scored mosaic classes shown in Figure 2L. *unc-40* animals expressing an unstable transgene with a *unc-40* rescuing construct, and cytoplasmic cell-specific markers in RIA and AIY, were scored for retention of the transgene and rescue of the AIY presynaptic phenotype. Four different classes of animals were scored: animals in which the transgene was retained in both AIY and RIA (D-F); 2) only in AIY but not in RIA (G-I); 3) only in RIA but not in AIY (J-L) or 4) animals not carrying the array (M-O). These animals were assayed for retention of the array (E, H, K, N; cell indicated in green) and distribution of presynaptic vesicles in the AIY interneuron (D, G, J, M). Scale bars, 5 μ m.

Suppl. Fig. 7 UNC-40/DCC acts cell-autonomously in RIA to control ventral RIA guidance. **(A)** *unc-40* animals expressing an unstable transgene with a *unc-40* rescuing construct, and cytoplasmic cell-specific markers in AIY and RIA were scored for retention of the transgene and rescue of the RIA ventral guidance phenotype. [***] notes significance of $p < 0.001$. **(B-C)** Expression in *unc-40*

animals of a bicistronic construct that contains the endogenous *unc-40* promoter driving the *unc-40* cDNA followed by a SL2 splice receptor and YFP. Expression of YFP in this bicistronic construct tracks *unc-40* endogenous expression, which was observed in several head neurons. Simultaneous cell-specific expression of a cytoplasmic fluorophore in RIA (white arrow) and RIB (B) demonstrated that UNC-40/DCC is endogenously expressed in RIA (C). (D-O) Confocal micrographs of representative animals belonging to the four scored mosaic classes. *unc-40* animals expressing an unstable transgene with an *unc-40* rescuing construct, and cytoplasmic cell-specific markers in RIA and AIY, were scored for retention of the transgene and rescue of the RIA guidance phenotype. Four different classes of animals were scored: animals in which the transgene was retained in both AIY and RIA (D-F); 2) only in RIA but not in AIY (G-I); 3) only in AIY but not in RIA (J-L) or 4) animals not carrying the array (M-O). These animals were assayed for retention of the array (E, H, K, N; cell indicated in green) and axon guidance in the RIA interneuron (D, G, J, M). Note that besides axon guidance, we also assayed presynaptic and postsynaptic site distribution in these animals by simultaneously visualizing glutamate receptors (GLR-1:YFP, pseudocolored red in D,G, J and M) and presynaptic vesicles (RAB-3:mCherry, pseudocolored green in E, H, K and N). Apart from axon guidance defects, the distribution in RIA of pre and postsynaptic sites was unaltered in *unc-40* mutants. Although RAB:mCherry was the same color as the cytoplasmic mCherry (used to track array retention), we could easily detect array retention in this background because of the difference in localization of the cytoplasmic fluorophore versus

the presynaptic RAB-3 vesicle marker (compare RIA cell bodies (circled in white) in E and H versus K and N). Scale bars, 5 μ m.

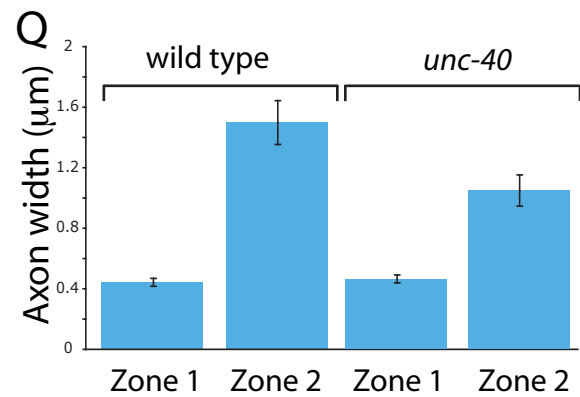
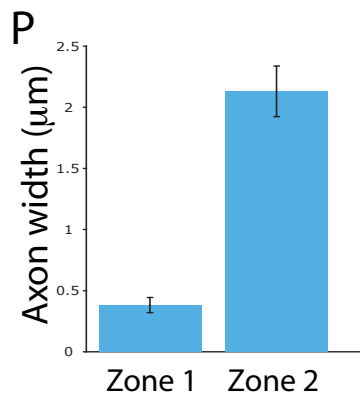
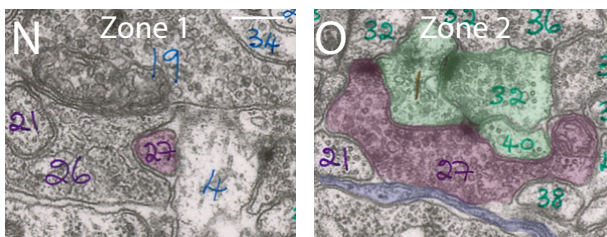
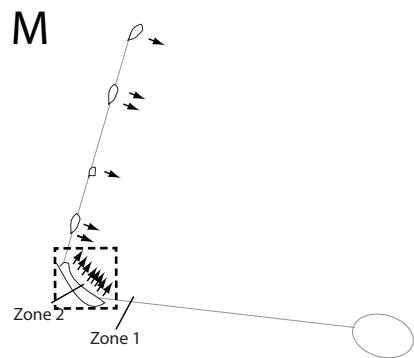
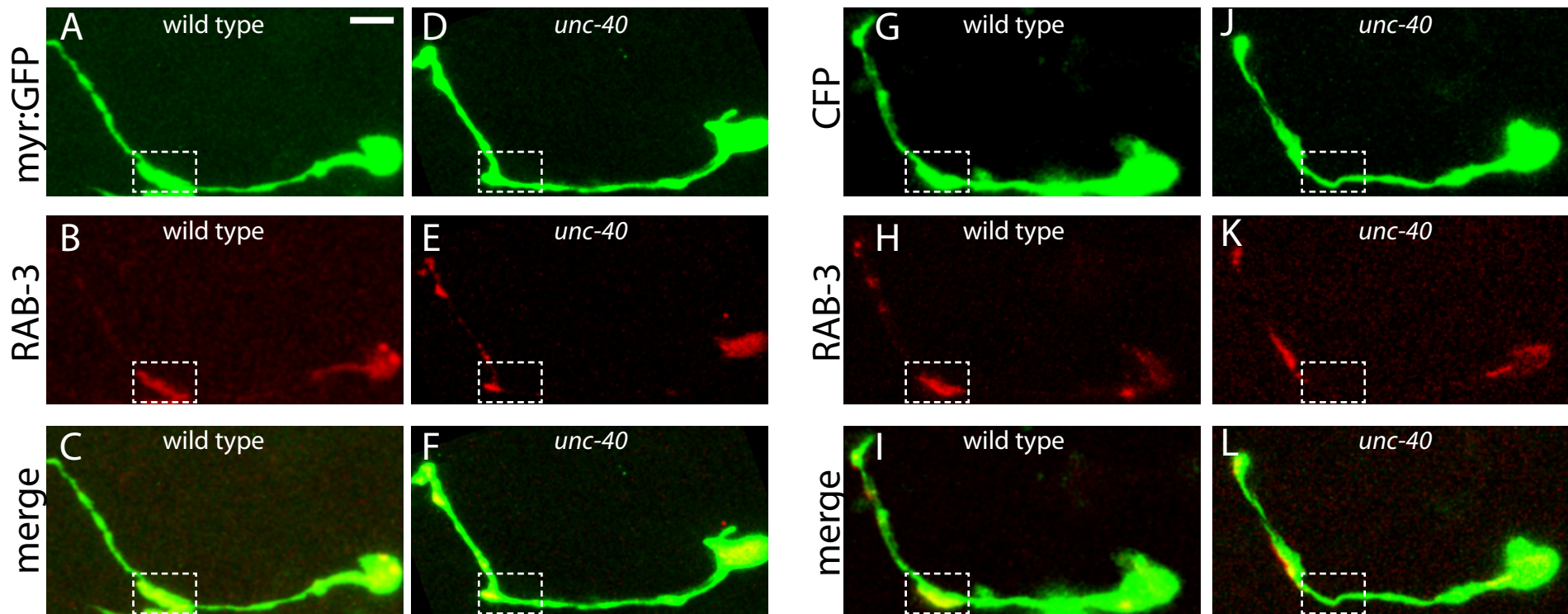
Suppl. Fig. 8 UNC-6/Netrin is required for correct presynaptic patterning in AIY.

(A) Confocal micrographs demonstrate the patterning of AIY presynaptic vesicles (GFP::*RAB-3* pseudocolored in red) in an *unc-6* animal. 71.9% of *unc-6* animals display a reduction of presynaptic sites at Zone 2 similar to that observed for *unc-40* animals (compare Suppl. Fig. 8A with Fig. 2F). Furthermore in 96.3% of *unc-6* animals, RIA neurons failed to make the ventral turn and meet AIY in Zone 2, phenocopying the defect observed in *unc-40* animals (n=107 animals and data not shown). It should be noted however that consistent with published results, we also observed other AIY defects in *unc-6* animals that were not observed in *unc-40* animals: 24.4% of animals had axon truncation and guidance defects, and 22.8% also had ectopic synapses in the normally asynaptic Zone 1 (data not shown). Because these two phenotypes are not observed in *unc-40* animals, they suggest that UNC-6/Netrin might play other UNC-40-independent roles at the nerve ring that affect AIY (32, 33). **(B)** *unc-6* animals expressing an unstable transgene with a *unc-6* rescuing construct, and cytoplasmic markers that expresses in ventral and dorsal cephalic sheath cells, were scored for retention of the transgene and rescue of the AIY presynaptic phenotype. Four different classes of animals were scored: 1) animals not carrying the transgene (V-C-); 2) animals in which the transgene was retained in both ventral (VCSC) and dorsal cephalic sheath cells (DCSC) (V+D+); 3) animals

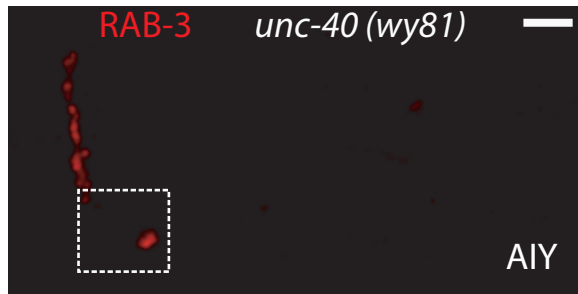
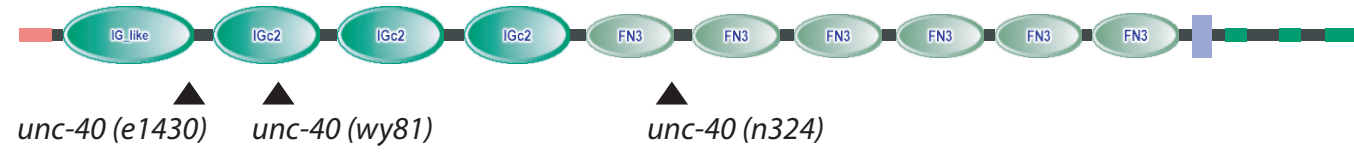
retaining the transgene in the VCSC but not in DCSC (V+D-); 4) and animals carrying the transgene but not having it in the VCSC (V-D+/-). Y axis represents percentage of animals with an AIY presynaptic defect. [***] notes significance of $p < 0.001$ between indicated groups. Scale bar, 5 μ m.

Suppl. Fig. 9 Position of sheath cells affects RIA guidance and AIY presynaptic patterning. **(A)** Quantification the positions of the sheath cell end-feet, RIA axon guidance and AIY presynaptic distribution in *unc-34* mutant animals (percentage of animals, n=94 animals). Note that 47.8% of *unc-34* animals have distended sheath cells. Of those animals, 41.5% had ectopic AIY presynaptic specializations in Zone 1, over the region of contact that overlapped the sheath cell. RIA guidance also changed accordingly but to a lesser degree: 21.2% of RIAs distended further posteriorly to the region covered by the sheath cell endfeet. The other 26.6% of RIAs did not project normally, but instead had axon truncations or abnormal projections that did not extend to Zone 2 (data not shown). The fact that these 26.6% of animals with abnormal RIA guidance still had ectopic synapses in AIY formed in Zone 1, over the region of contact with the sheath cells, is consistent with our mosaic analysis and supports the hypothesis that the presynaptic sites in AIY are directed by the sheath cells and not the RIA postsynaptic partner. **(B-D)** Presynaptic vesicles in AIY, labeled using GFP::RAB-3 and pseudocolored red in *unc-34* animals (B), *unc-40* animals (C) or *unc-34;unc-40* animals (D). Note that the double mutant (D) phenocopies *unc-40* animals (C) (n>200, 100% penetrant). These epistasis data show that the

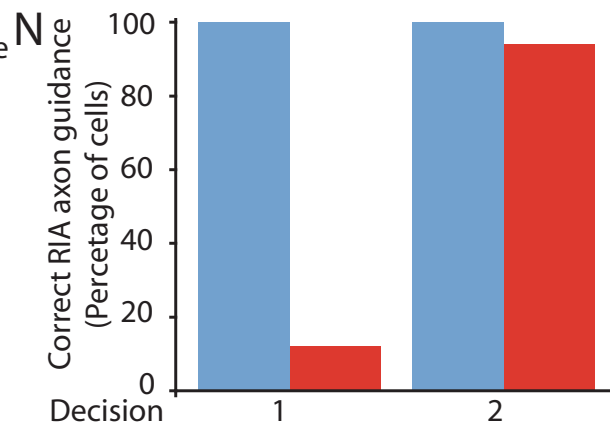
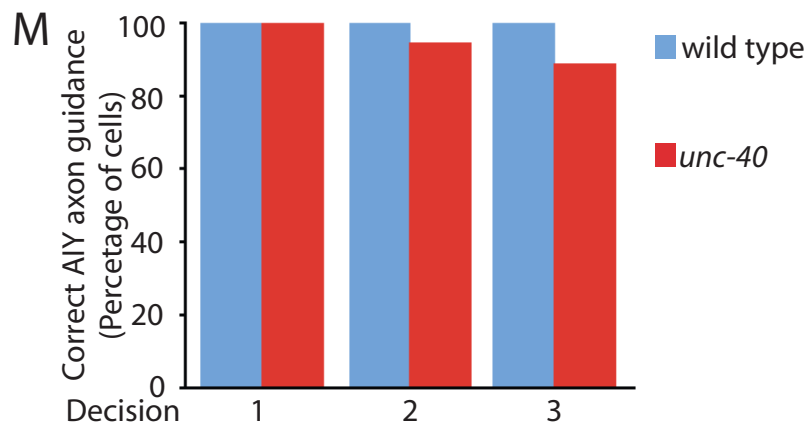
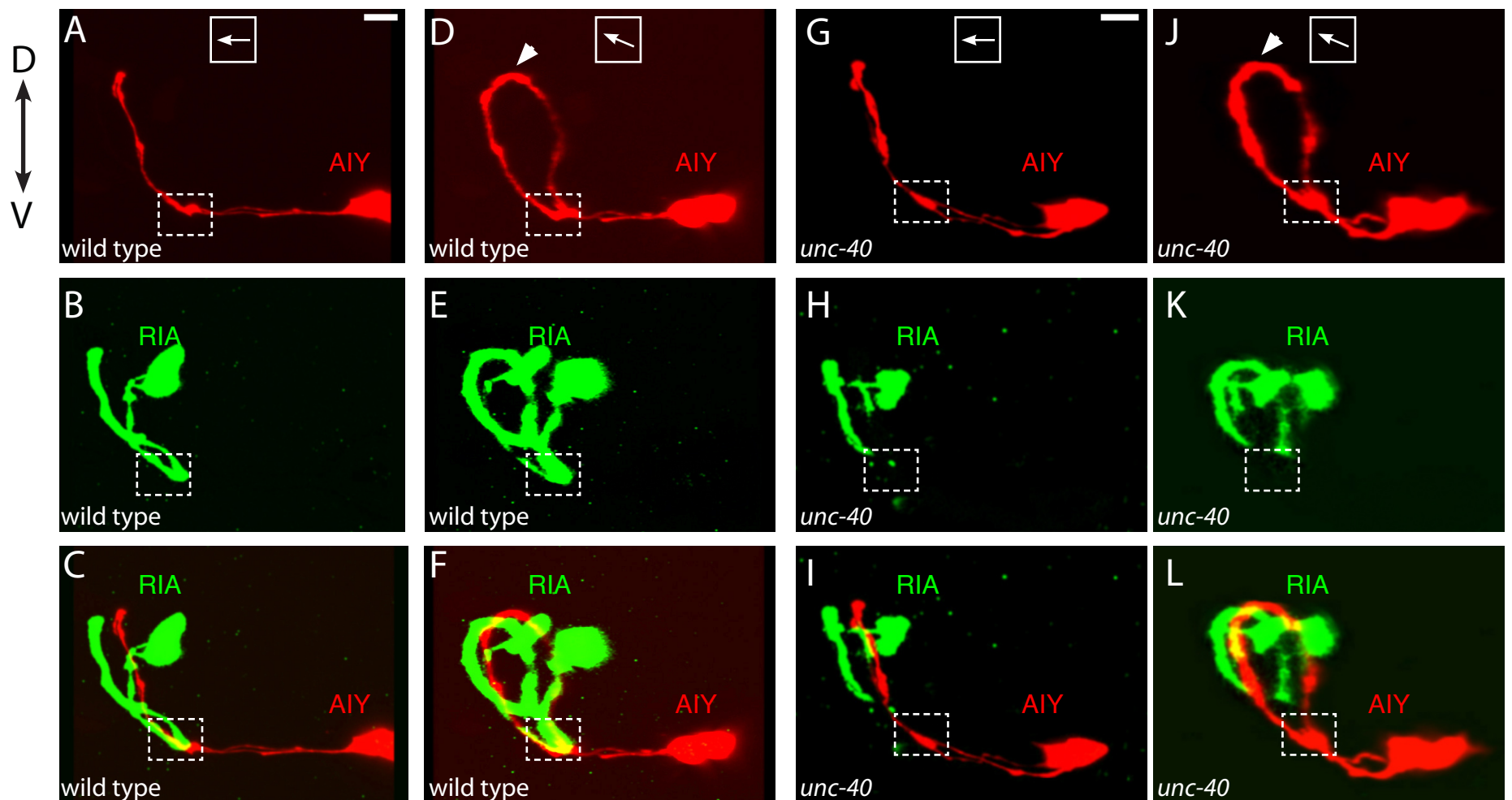
displacement of presynaptic sites observed in *unc-34* animals is an UNC-40/DCC-dependent event, consistent with a model whereby UNC-34/Enabled affects presynaptic patterning in AIY by altering sheath cell morphology, which then affects localized UNC-6/Netrin secretion, UNC-40/DCC localization and presynaptic assembly. Scale bars, 5 μ m.



Sup. Figure 1

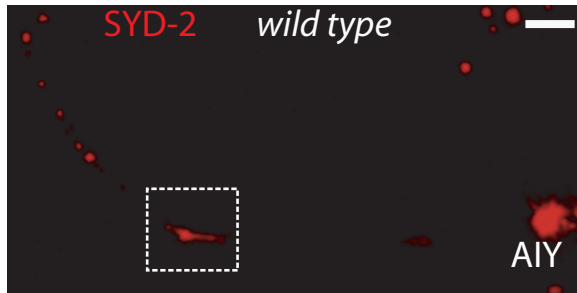
A**B**

Sup. Figure 2



Sup. Figure 3

A

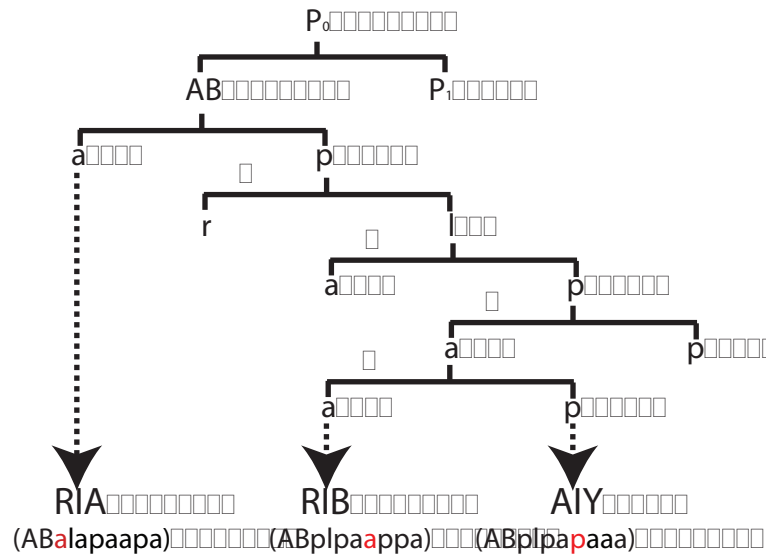


B



Sup. Figure 4

A

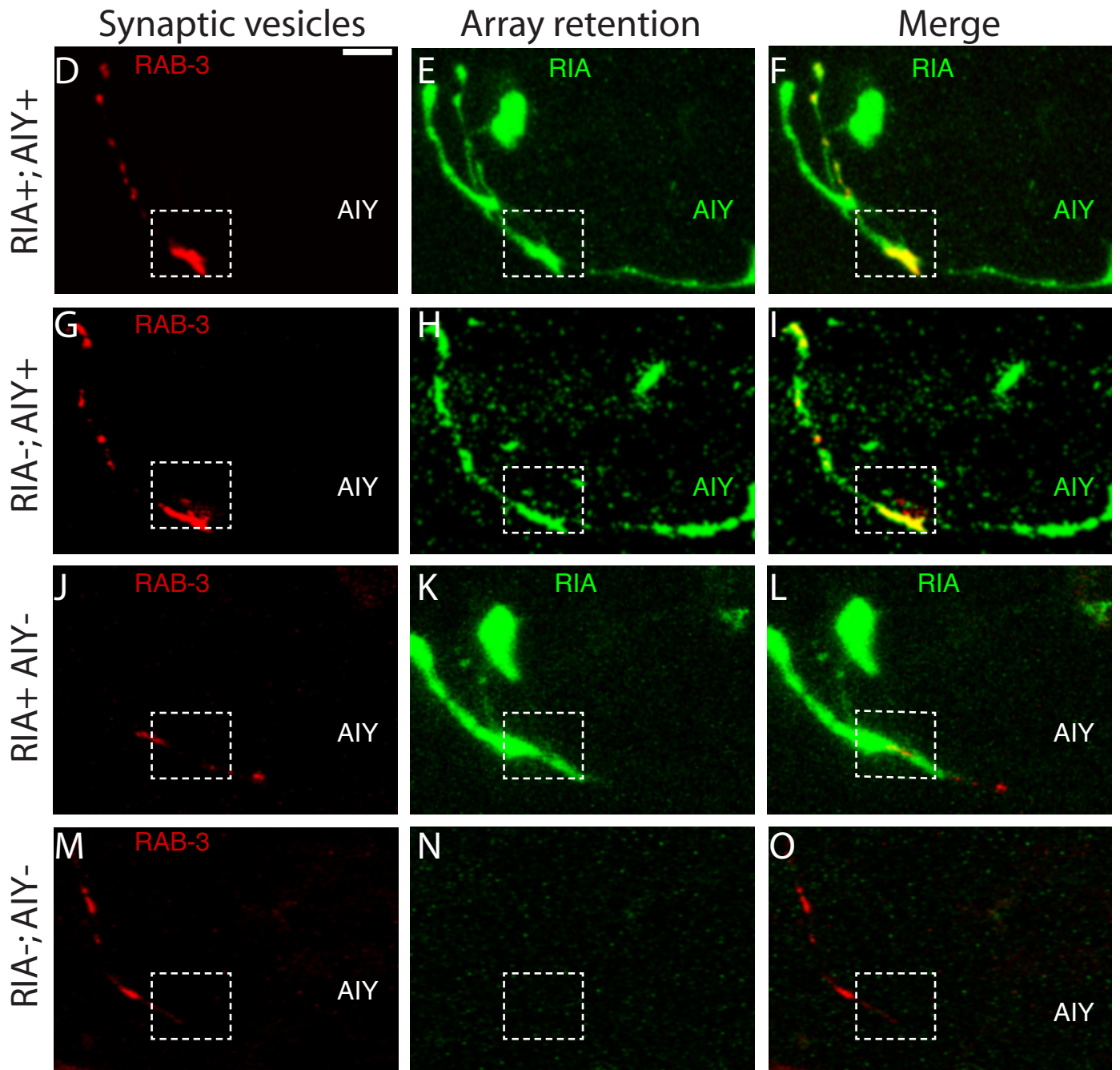
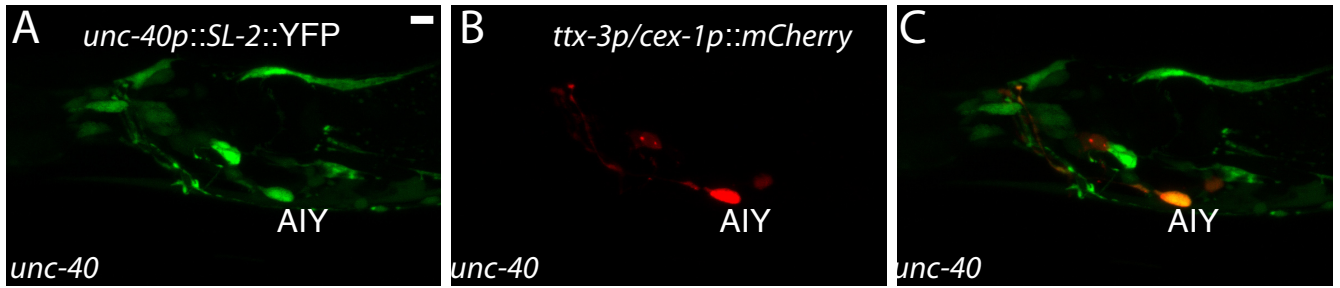


B

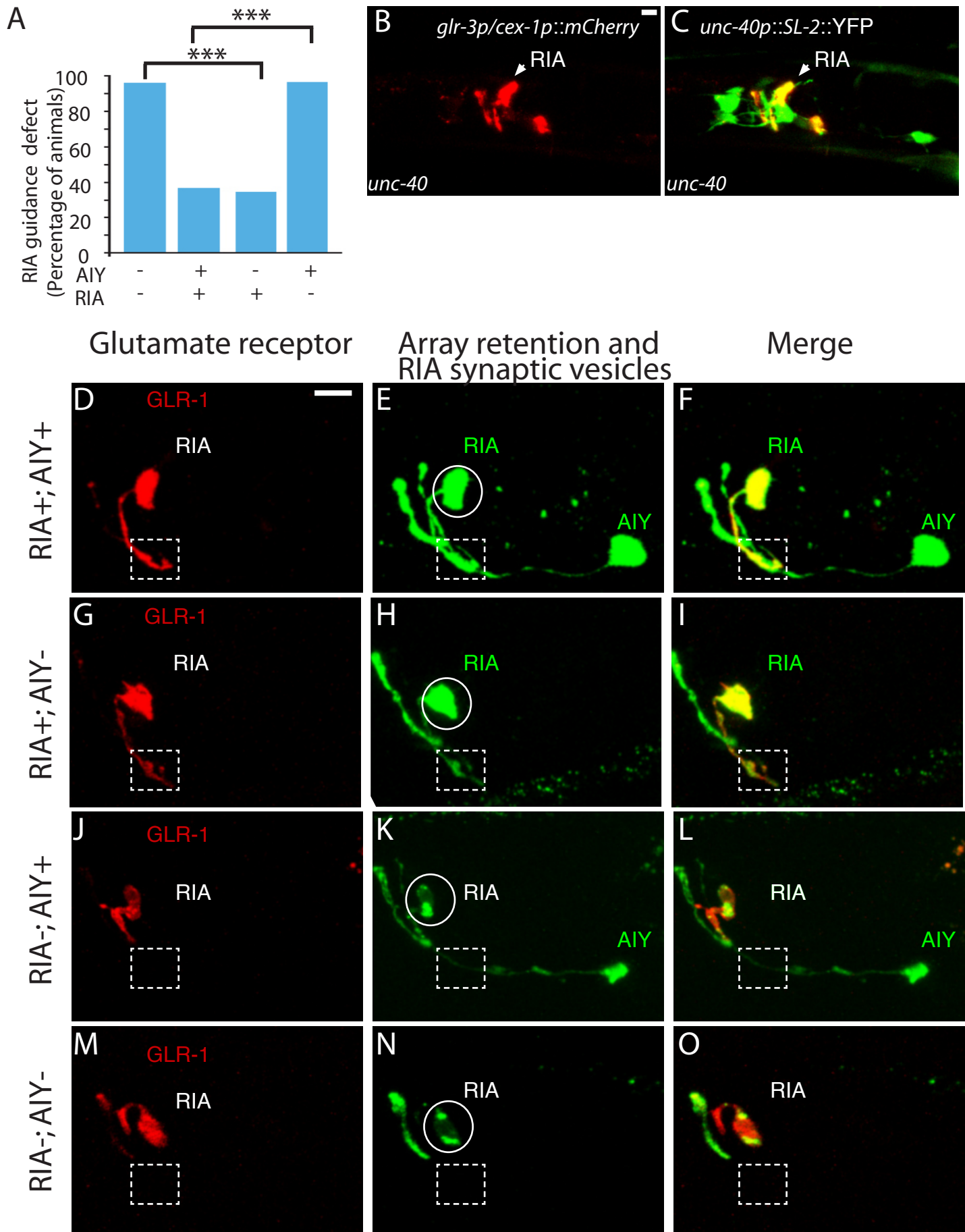
	Head	Zone 2 region
Rectal epithelium D	-	-
PVT	X	-
K'	-	-
DVB	-	-
Rectal hyp.	-	-
Excretory cell	-	-
RMEV	X	X
DB5	-	-
SI AVL	X	-
AVKL	X	-
Excretory gland L	X	-
SIBVL	X	-
SIADL	X	-
SMDDL	X	-
AIYL	X	X

C

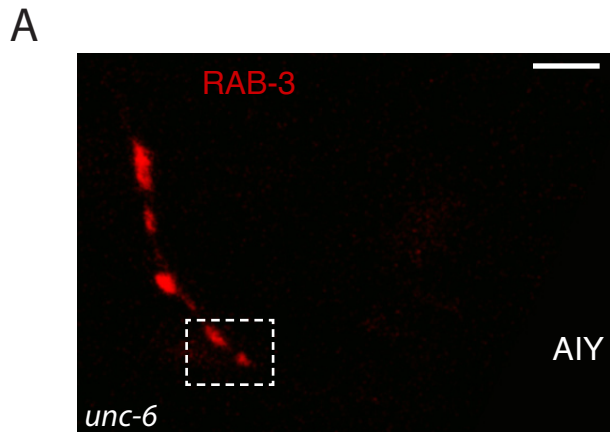
	Head	Zone 2 region
virL	-	-
virR	-	-
AVG	-	-
RIR	X	-
RIS	X	-
AVL	X	-
RIH	X	X
DB4	-	-
SI AVR	X	-
AVKR	X	-
Excretory gland R	X	-
SIBVR	X	-
SIADR	X	-
SMDDR	X	-
DA8	-	-
AIYR	X	X



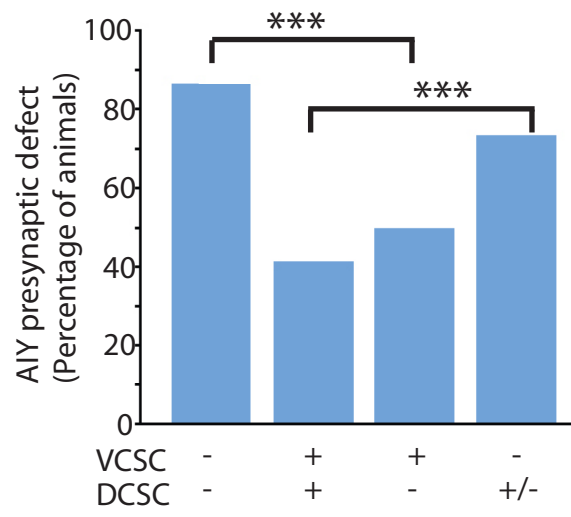
Sup. Figure 6



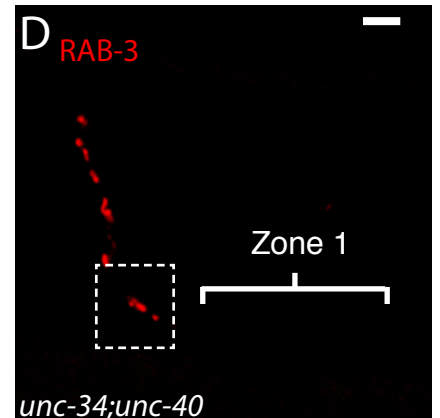
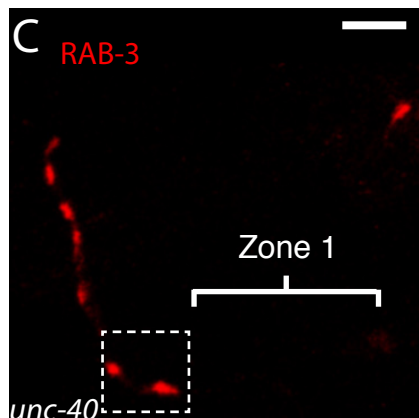
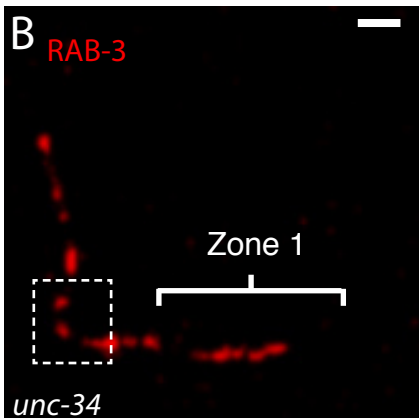
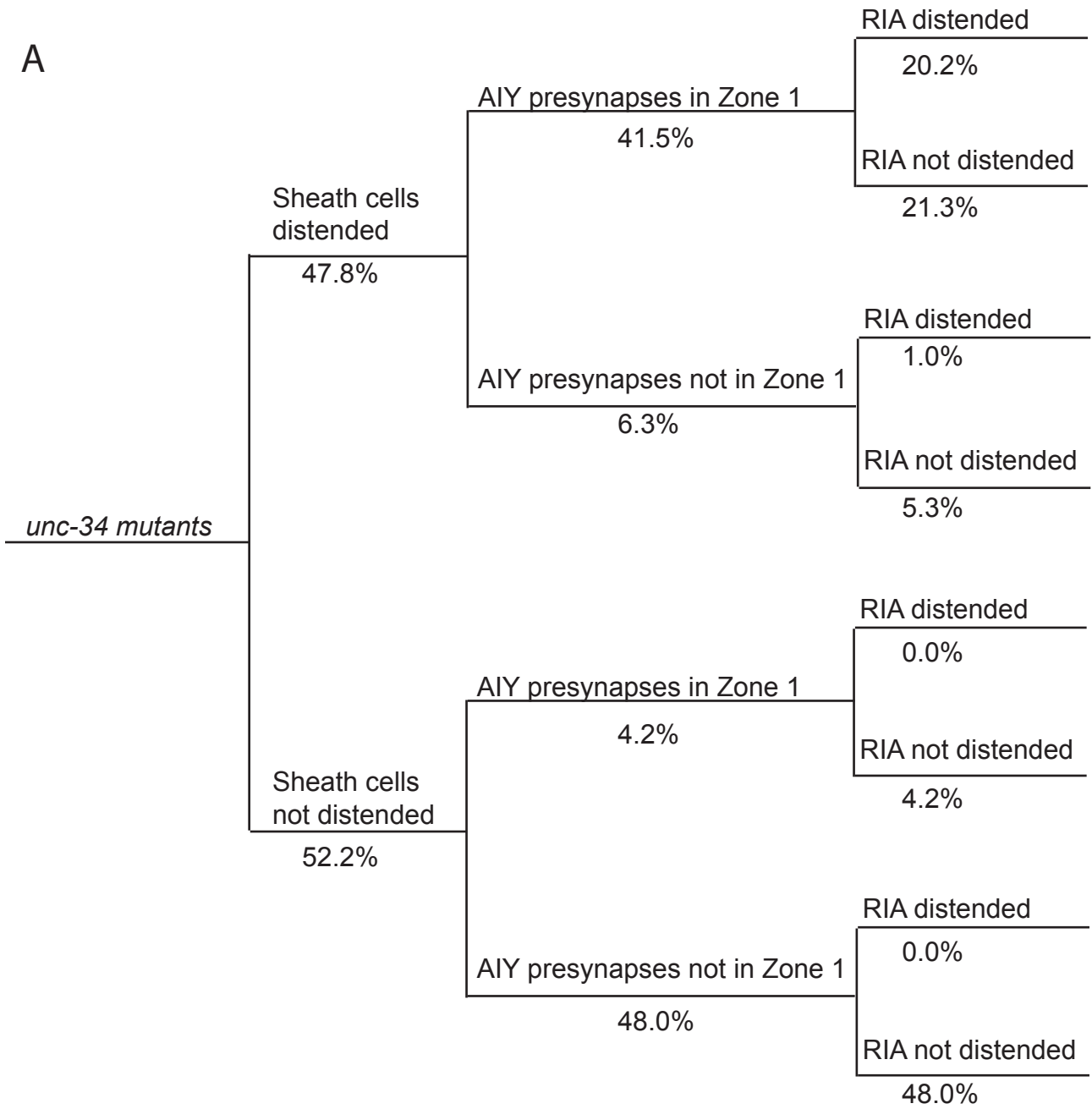
Sup. Figure 7



B



Sup Figure 8



Sup. Figure 9